Vorticity in peripheral collisions at the Facility for Antiproton and Ion Research and at the JINR Nuclotron-based Ion Collider fAcility

L. P. Csernai,[1] D. J. Wang,[1] M. Bleicher,[2,3] and H. Stöcker[2,3,4]

[1]*Institute of Physics and Technology, University of Bergen, Allegaten 55, 5007 Bergen, Norway*
[2]*Frankfurt Institute for Advanced Studies - Goethe University, 60438 Frankfurt am Main, Germany*
[3]*Institut für Theoretische Physik, Goethe Universität, 60438 Frankfurt, Am Main, Germany*
[4]*GSI Helmholtzzentrum für Schwerionenforschung GmbH, Planckstr. 1, 64291 Darmstadt, Germany*

The flow vorticity development is studied in the reaction plane of peripheral relativistic heavy-ion reactions at energies just above the threshold of the transition to a quark-gluon plasma (QGP). Earlier calculations at higher energies with larger initial angular momentum predicted significant vorticity leading to measurable Λ polarization. Here we discuss the possibility of vorticity and circulation in dense plasma at lower temperatures. In low-viscosity QGP this vorticity still remains significant.

Fluid dynamical processes in heavy-ion reactions were studied for a long time [1–3], and their use is becoming more dominant in recent years. With the quark-gluon plasma (QGP) production in these reactions, the scope of the fluid dynamical studies is widening at the same time [4]. As in the present studies, both different fluctuating modes and global collective processes lead to flow observables, so it becomes important to separate or split the two types of flow processes from each other [5,6]. This separation would help the precise analysis of both processes.

In peripheral heavy-ion reactions due to the initial angular momentum, the initial state of the fluid dynamical stage of the collision dynamics has shear flow characteristics, and this leads to rotation [7] and even the Kelvin–Helmholtz instability (KHI) [8] in the reaction plane for a low-viscosity quark-gluon plasma. This possibility was indicated by high-resolution computational fluid dynamics (CFD) calculations using the Particle in Cell (PIC) method. We study the development of these processes in a $(3+1)$-dimensional $(3+1)$D configuration to describe the energy and momentum balance realistically. The presently used relativistic PICR hydro was the first, which included the QGP equation of state (EoS) [9], the y and p_t spectra were evaluated and the softening of the EoS was predicted in 1994, leading to a strong change of $p_x(y)/a$ [or $v_1(y)$], [10–12], which led to the prediction of the third flow component or antiflow [13]. This was then measured at the BNL Relativistic Heavy-Ion Collider (RHIC) and presented in 2006 [14]. Just as in the publications discussing the RHIC (including the Beam Energy Scan) results [15–18], here we also used the initial-state model assuming transparency and strong attractive fields with accurate impact-parameter dependence and rapidity distribution in the transverse plane [19]. This initial-state model is used as for all configurations assuming transparency and QGP. It assumes an initial interpenetration of Lorentz-contracted slabs (in most present models considered as Color Glass Condensate), and strong attractive coherent Yang–Mills fields act between these end slabs, with large string tension (according to the color rope model [20]). During the slowing down of these expanding fields the original net baryon charge is considered to be longitudinally uniformly distributed in the streak-by-streak expanding system and then, in the subsequent initial Riemann scaling expansion, the net baryon charge follows this expansion.

In this work we study the development of vorticity in high-energy heavy-ion reactions just above the phase-transition threshold, where the viscosity is estimated to have a minimum, so the viscous dissipation is small [21,22], and the spherical expansion is also smaller due to the lower pressure, thus the initial local rotation, the vorticity becomes slower.

In Ref. [23] it was found that, at Large Hadron Collider (LHC) and RHIC energies, the angular momentum in peripheral collisions reaches $-L_y = 10^6 \hbar$ and the relativistic vorticity averaged over all layers parallel to the reaction plane reaches $3\,c/\text{fm}$. This is more than an order of magnitude higher than the vorticity from random fluctuations in the transverse plane [24]. There, the initial average vorticity, ω_1, is $\sim 0.2\,c/\text{fm}$ and drops to 0.11 (0.06) c/fm at fluid dynamical expansion times of $t = 3.56\,(6.94)$ fm/c in the parallel propagation case.

For the dynamical initial state, a Yang–Mills field theoretical model [19] used in Ref. [23] considered a longitudinal expansion lasting 4 fm/c from the initial impact, which should be added to the previously mentioned fluid dynamical expansion times.

This type of initial state is described in great detail in Ref. [19]. In our present fluid dynamical calculation we use this initial-state model, which is tested in several model calculations in the last decade. It describes correctly the initial shear flow characteristics. The initial angular momentum is based on the assumption that the initial angular momentum of the participants (based on straight propagation geometry) is streak-by-streak conserved, thus our model satisfies angular momentum conservation both locally and globally.

Figure 1 shows the vorticity projected to the reaction plane for a collision for a collision energy of the Nuclotron-based Ion Collider fAcility (NICA) at the Joint Institute for Nuclear Research in Dubna, Russia, $\sqrt{s_{NN}} = 4.65 + 4.65$ GeV, at an initial moment of time and at a later time. The peak value of the vorticity is a few times smaller than at the ultrarelativistic RHIC and LHC energies, but the negative values are less pronounced. The initial state is the same as
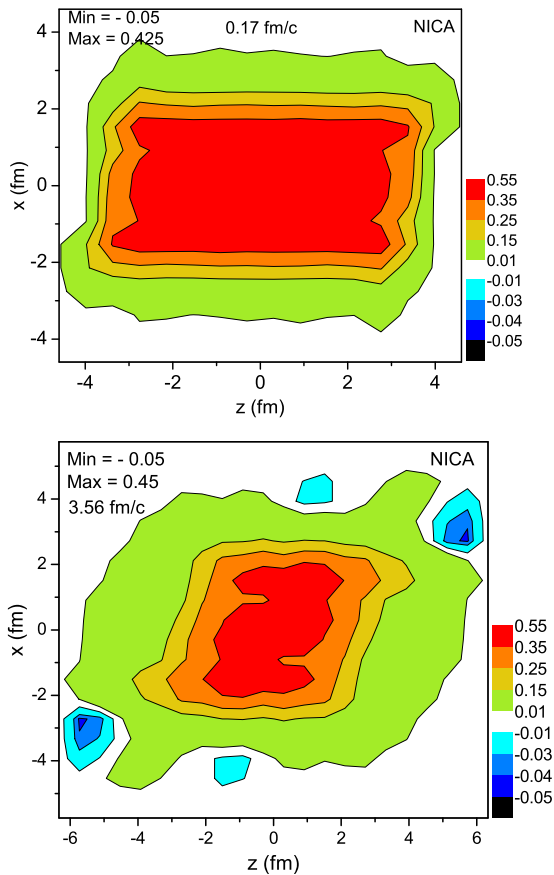
FIG. 1. (Color online) The classical weighted vorticity Ω_{zx}, calculated in the reaction [x-z] plane at $t = 0.17$ fm/c and at $t = 3.56$ fm/c. The energy of the Au + Au collision is $\sqrt{s_{NN}} = 4.65 + 4.65$ GeV, $b = 0.5 b_{\max}$, and the cell size is $dx = dy = dz = 0.575$ fm. The average vorticity Ω_{zx} is 0.1345 and 0.0773 c/fm for the two selected times, respectively. The vorticity in the other directions is significantly weaker.

the one that was used at high energy: we assume transparency, QGP formation, initial longitudinal expansion in the same Yang–Mills string-rope model for 4 fm/c time. At the later time the drop of the vorticity is not as large as at the higher energies, because of the less explosive expansion.

Similarly to Ref. [23] we evaluate first the classical vorticity in the reaction plane [x-z], defined as

$$\omega_y \equiv \omega_{xz} \equiv -\omega_{zx} \equiv \tfrac{1}{2}(\partial_z v_x - \partial_x v_z), \tag{1}$$

where the x, y, z components of the three-velocity v are denoted by v_x, v_y, v_z, respectively.

We also define an energy-density-weighted average vorticity as [23]

$$\Omega_{zx} \equiv \sum_{ik}^{N_{\text{cell}}} \frac{E_{ik}}{(E_{\text{tot}}/N_{\text{cell}})} \, \omega_{zx}(ik), \tag{2}$$

so that this weighting does not change the average circulation of the layer, i.e., the sum of the average of the weights over all fluid cells is unity: $\langle w(z,x) \rangle = 1$. The total energy content
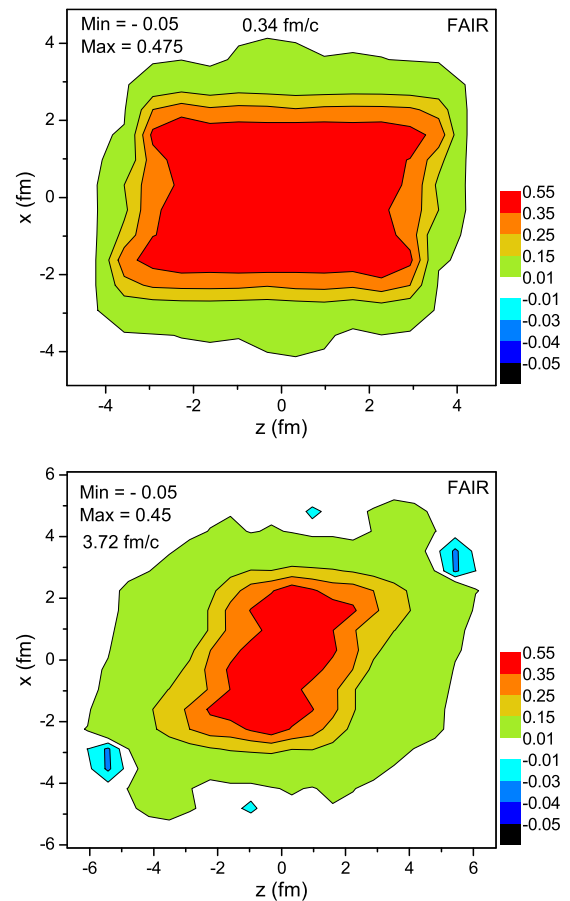

FIG. 2. (Color online) The classical weighted vorticity Ω_{zx}, calculated in the reaction [x-z] plane at $t = 0.34$ fm/c and $t = 3.72$ fm/c. The energy of the U + U collision is $\sqrt{s_{NN}} = 4.0 + 4.0$ GeV, $b = 0.5 b_{\max}$, and the cell size is $dx = dy = dz = 0.610$ fm. The average vorticity Ω_{zx} is 0.1297 and 0.0736 c/fm for the two selected times, respectively.

of a cell at point (z,x) or that corresponding to the grid index i,k is $E_{ik} = T^{00}(z,x)$. The total energy in a y layer (or in all y layers) is $E_{\text{tot}} = \sum_{ik} E_{ik}$, while the number of cells is in a y layer (or in all y layers) is N_{cell}.

In Fig. 2 the vorticity projected to the reaction plane for a collision for the Facility for Antiproton and Ion Research (FAIR) energy of $\sqrt{s_{NN}} = 4.0 + 4.0$ GeV is shown at an initial moment of time and at a later time. The peak value of the vorticity is similar to the previous example—a few times smaller than at the ultrarelativistic RHIC and LHC energies—but the negative values are less pronounced. We also assume transparency, QGP formation, and initial longitudinal expansion in the same Yang–Mills string-rope model for 4 fm/c time.

In these lower-energy reactions we did not observe significant formation of the KHI, although QGP formation was assumed and low viscosity (i.e., only the numerical viscosity as in the high-energy calculations).

These results are promising: if QGP is formed in these reactions then the rotation may be still observable at NICA and FAIR energies.

If the energy at these accelerators is not sufficient to achieve QGP formation then the larger hadronic pressure will lead to earlier and more rapid expansion so, although the angular momentum will have to be the same, the rotational energy will be reduced faster and converted into more explosive expansion. In this case we have considerably less chance to observe the consequences of rotation and vorticity. In addition the viscosity of the system will also be considerably larger, which will lead to the dissipation of the local rotation (vorticity) and hinder the buildup of the uniform rotation from the original stratified shear flow configuration.

Because significant KHI was not present in the QGP flow configurations at these energies, the KHI is even less probable to occur for the stiffer and more viscous hadronic matter.

Note that directed flow measurements showed the signs of the phase transition to QGP at the threshold, and the beam-energy dependence of this effect was studied recently at RHIC [25]. We have to mention that the rotation also influences the directed flow, and it leads to a decrease of the amplitude of v_1 with increasing energies [7,26]. This change may even lead to the reversal of antiflow to directed flow if the initial angular momentum and consequently the rotation are strong enough.

In addition to the directed flow (v_1) [7,26], two methods were proposed so far to detect the effects of rotation the differential Hanbury Brown and Twiss (HBT) method [27] and the polarization of emitted fermions based on the equipartition of the rotation between the spin and orbital degrees of freedom [28,29].

The differential HBT method is a global, integral observable, so it can detect well the rotation of the system. On the other hand, the absence of the KHI will slow down the formation of uniform rotation of the system, and the original stratified shear flow may persist for a longer time. This will make the differential HBT method more dependent on the angle of observation, and to select the effects of azimuthal HBT [30], and differential HBT will become more involved.

The particle-polarization effect has some advantages and disadvantages. The local polarization depends on the thermal vorticity [28,29]. Now at lower collision energy the temperature is lower and the thermal vorticity increases, which is advantageous. At ultrarelativistic energies this feature led to the conclusion that the predicted polarization is bigger for RHIC than for LHC, because of the lower temperature of the system.

The thermal vorticity occurs in polarization studies because the spin-orbit interaction aligns the spins and the orbital momentum, while the random thermal motion works against this alignment. Thus we use the the inverse-temperature four-vector field [28,29],

$$\beta^\mu(x) = [1/T(x)]u^\mu(x),$$

and define the *thermal vorticity* as

$$\varpi^{\mu\nu} = \tfrac{1}{2}(\partial^\nu \hat{\beta}^\mu - \partial^\mu \hat{\beta}^\nu), \qquad (3)$$

where $\hat{\beta}^\mu \equiv \hbar \beta^\mu$. Thereby, ϖ becomes dimensionless.

TABLE I. Time dependence of average vorticity projected to the reaction plane for heavy-ion reactions at the NICA energy of $\sqrt{s_{NN}} = 4.65 + 4.65$ GeV.

t (fm/c)	Vorticity (classical) (c/fm)	Thermal vorticity (relativistic) (1)
0.17	0.1345	0.0847
1.02	0.1238	0.0975
1.86	0.1079	0.0846
2.71	0.0924	0.0886
3.56	0.0773	0.0739

In Ref. [28] for a Au + Au collision at $\sqrt{s_{NN}} = 200$ GeV, $b = 0.7 \, b_{\max}$, the cell size is $dx = dy = dz = 0.4375$ fm, and the average weighted thermal vorticity is $\langle \Omega_{zx} \rangle = 0.0453$. This led to a nearly 10% polarization for Λs and $\bar{\Lambda}$s, emitted in the reaction plane, in the x direction at the event-by-event center-of-mass (c.m.) rapidity.

At the NICA and FAIR lower energies the at the same time the average weighted thermal vorticity is significantly larger, 0.0739 and 0.0658 respectively. See Tables I and II. The average thermal vorticity first increases and then decreases due to the rotation of the expanding system, which is showed in our recent study [31]. The thermal vorticity projected to the reaction plane is shown in Figs. 3 and 4.

On the other hand, at lower energies we have a problem; namely, that the multiplicity of Λs and $\bar{\Lambda}$s is considerably less than at the higher energies and other higher-multiplicity particles must be used to determine the polarization of the emitting source.

For us the rate of this decrease is important, to see if we can still detect the vorticity and circulation at freeze-out. Notice that we calculated only the Ω_{zx} component of the weighted vorticity distributions. Due to the close-to-spherical expansion, the direction of vorticity may develop into different directions.

An analysis of the vorticity development was performed for peripheral Au + Au reactions at NICA and U + U reactions at FAIR energies of $\sqrt{s_{NN}} = 9.3/8.0$ GeV. The initial peak vorticity was about two times larger than the one obtained from random fluctuations in the transverse plane, of about 0.2 c/fm at much higher energies [24]. The reason is in the

TABLE II. Time dependence of average vorticity projected to the reaction plane for heavy-ion reactions at the FAIR energy of $\sqrt{s_{NN}} = 4.0 + 4.0$ GeV.

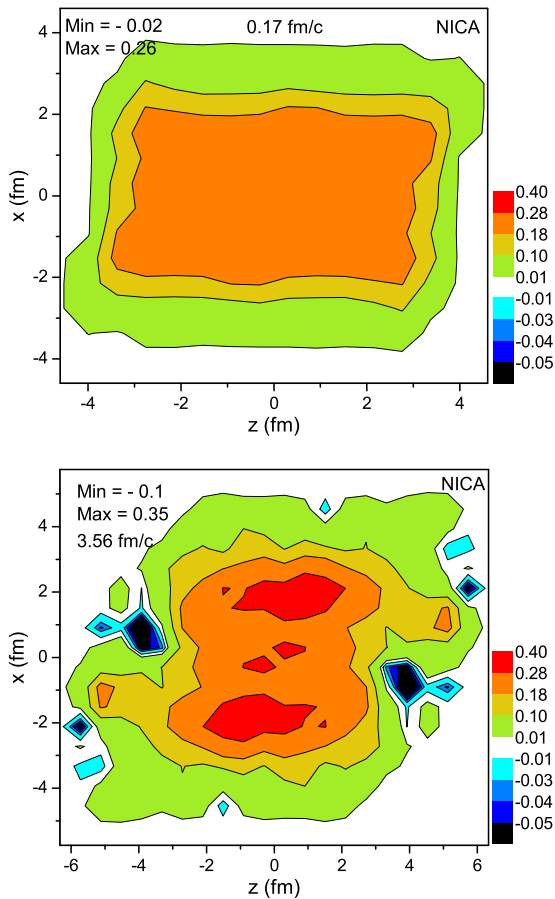| t (fm/c)	Vorticity (classical) (c/fm)	Thermal vorticity (relativistic) (1)
0.34	0.1297	0.0846
2.03	0.1020	0.0866
3.72	0.0736	0.0658
5.42	0.0520	0.0515
7.11	0.0377	0.0426

FIG. 3. (Color online) The relativistic weighted thermal vorticity Ω_{zx}, calculated in the reaction [x-z] plane at $t = 0.17$ fm/c and at $t = 3.56$ fm/c. The energy of the Au + Au collision is $\sqrt{s_{NN}} = 4.65 + 4.65$ GeV, $b = 0.5b_{max}$, and the cell size is $dx = dy = dz = 0.575$ fm. The average thermal vorticity Ω_{zx} is 0.0847 and 0.0739 for the two selected times, respectively. The thermal vorticity decreases much slower than the standard vorticity due to the decreasing temperature.

FIG. 4. (Color online) The relativistic weighted thermal vorticity Ω_{zx}, calculated in the reaction [x-z] plane at $t = 0.34$ fm/c and at $t = 3.72$ fm/c. The energy of the U + U collision is $\sqrt{s_{NN}} = 4.0 + 4.0$ GeV, $b = 0.5b_{max}$, and the cell size is $dx = dy = dz = 0.610$ fm. The average vorticity Ω_{zx} is 0.0856 and 0.0658 for the two selected times, respectively.

initial angular momentum arising from the beam energy in noncentral collisions.

In this work we repeat the earlier model studies [23], leading to the mentioned observable signatures related to the (rapidity-odd component) of the directed flow, which is a promising possibility for the observations [32].

The vorticity reaches a maximum soon after local equilibration when the rotation equilibrates in the system. Although the vorticity decreases rapidly due to the explosive expansion of the system, still, at ~4 fm/c after the beginning of fluid dynamical expansion, the peak vorticity is still above the value arising from random fluctuations.

The thermal vorticity is even larger than the estimated value at LHC and RHIC energies, which makes polarization studies promising in this lower-energy domain. At the same time other detection methods should be worked out because the use of Λ and $\bar{\Lambda}$ polarization is not applicable at low energies due to the low multiplicity of these particles.

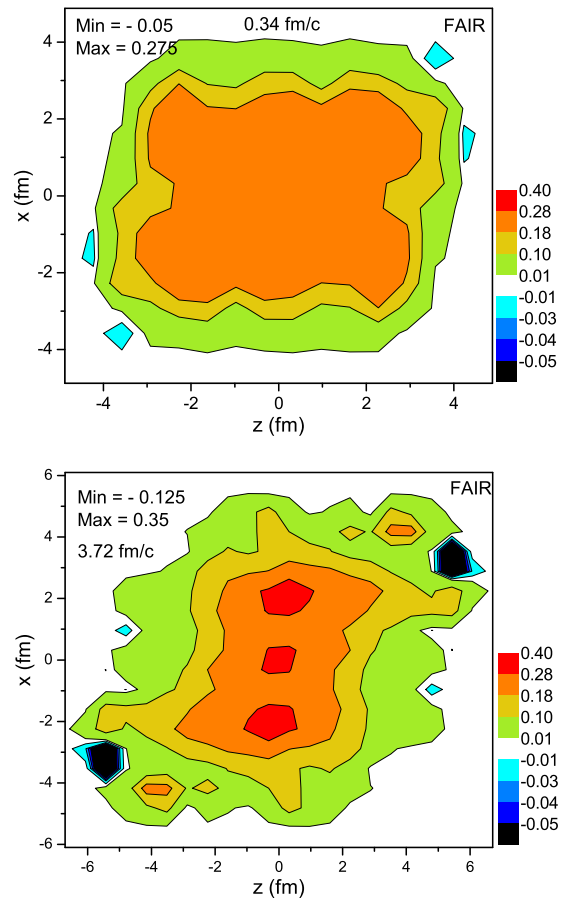At GSI the planned facilities, e.g., at PANDA [33], will make it possible to measure proton and antiproton polarization in the emission directions where significant polarization is expected.

Similar studies were performed recently [34,35], for the chiral vortaic effect in the QGSM approach. Also significant signals are expected, although the dominant signal is different from the one predicted in our model. In our model the vorticity is directed in the $-y$ direction (i.e., orthogonal to the reaction plane) and the result is maximum transverse polarization for particles emitted in the $(+/-)$ x direction (i.e., in the reaction plane), while the polarization of particles emitted into the $(+/-)$ y direction is negligible. In the case of chiral vortaic effect with time significant helicity enhancement is expected for particles emitted in the $(+/-)$ y direction. There are certainly differences in the dynamics of the used models, thus it will be interesting to see which of these are supported by the experiments.

[1] H. Stöcker, L. P. Csernai, G. Graebner, G. Buchwald, H. Kruse, R. Y. Cusson, J. A. Maruhn, and W. Greiner, Phys. Rev. C **25**, 1873 (1982).

[2] L. P. Csernai and J. I. Kapusta, Phys. Rep. **131**, 223 (1986).

[3] H. Stöcker and W. Greiner, Phys. Rep. **137**, 277 (1986).

[4] H. Stöcker, Nucl. Phys. A **750**, 121 (2005).

[5] L. P. Csernai and H. Stöcker [J. Phys. G (to be published)], arXiv:1406.1153.

[6] S. Floerchinger and U. A. Wiedemann, Phys. Rev. C **88**, 044906 (2013).

[7] L. P. Csernai, V. K. Magas, H. Stöcker, and D. D. Strottman, Phys. Rev. C **84**, 024914 (2011).

[8] L. P. Csernai, D. D. Strottman, and Cs. Anderlik, Phys. Rev. C **85**, 054901 (2012).

[9] Sz. Horvát, V. K. Magas, D. D. Strottman, and L. P. Csernai, Phys. Lett. B **692**, 277 (2010).

[10] L. V. Bravina, N. S. Amelin, L. P. Csernai, P. Lévai, and D. Strottman, Nucl. Phys. A **566**, 461 (1994).

[11] D. Strottman, Nucl. Phys. A **566**, C245 (1994).

[12] L. Bravina, L. P. Csernai, P. Lévai, and D. Strottman, Phys. Rev. C **50**, 2161 (1994).

[13] L. P. Csernai and D. Röhrich, Phys. Lett. B **458**, 454 (1999).

[14] Gang Wang (STAR Collaboration), Nucl. Phys. A **774**, 515 (2006).

[15] D. J. Wang, L. P. Csernai, D. Strottman, Cs. Anderlik, Y. Cheng, D. M. Zhou, Y. L. Yan, X. Cai, and B. H. Sa, Eur. Phys. J. A **48**, 168 (2012).

[16] L. P. Csernai, A. Skalvik, D. J. Wang, D. Strottman, C. Anderlik, Y. Cheng, Y. L. Yan, and B. H. Sa, Cent. Eur. J. Phys. **10**, 1271 (2012).

[17] L. P. Csernai, A. M. Skålvik, D. J. Wang, V. K. Magas, H. Stöcker, D. D. Strottman, Y. Cheng, and Y. L. Yan, Acta Phys. Pol. B **43**, 803 (2012).

[18] Yu-Liang Yan, Yun Cheng, Dai-Mei Zhou, Bao-Guo Dong, Xu Cai, Ben-Hao Sa, and L. P. Csernai, J. Phys. G **40**, 025102 (2013).

[19] V. K. Magas, L. P. Csernai, and D. D. Strottman, Phys. Rev. C **64**, 014901 (2001); Nucl. Phys. A **712**, 167 (2002).

[20] T. S. Biró, H. B. Nielsen, and J. Knoll, Nucl. Phys. B **245**, 449 (1984).

[21] P. K. Kovtun, D. T. Son, and A. O. Starinets, Phys. Rev. Lett. **94**, 111601 (2005).

[22] L. P. Csernai, J. I. Kapusta, and L. D. McLerran, Phys. Rev. Lett. **97**, 152303 (2006).

[23] L. P. Csernai, V. K. Magas, and D. J. Wang, Phys. Rev. C **87**, 034906 (2013).

[24] S. Floerchinger and U. A. Wiedemann, J. High Energy Phys. 11 (2011) 100; J. Phys. G: Nucl. Part. Phys. **38**, 124171 (2011).

[25] Adamczyk *et al.* (STAR Collaboration), arXiv:1401.3043.

[26] J. Steinheimer, J. Auvinen, H. Petersen, M. Bleicher, and H. Stöcker, Phys. Rev. C **89**, 054913 (2014).

[27] L. P. Csernai, S. Velle, and D. J. Wang, Phys. Rev. C **89**, 034916 (2014); L. P. Csernai and S. Velle, Int. J. Mod. Phys. E **23**, 1450043 (2014).

[28] F. Becattini, L. P. Csernai, and D. J. Wang, Phys. Rev. C **88**, 034905 (2013).

[29] F. Becattini, V. Chandra, L. Del Zanna, and E. Grossi, Ann. Phys. (NY) **338**, 32 (2013).

[30] G. Graef, M. Bleicher, and M. Lisa, Phys. Rev. C **89**, 014903 (2014).

[31] L. P. Csernai, D. J. Wang, and T. Csörgö, Phys. Rev. C **90**, 024901 (2014).

[32] L. P. Csernai, G. Eyyubova, and V. K. Magas, Phys. Rev. C **86**, 024912 (2012).

[33] Alaa Dbeyssi, **PoS** (Bormio 2013) 059.

[34] M. Baznat, K. Gudima, A. Sorin, and O. Teryaev, Phys. Rev. C **88**, 061901 (2013).

[35] O. V. Rogachevsky, A. S. Sorin, and O. V. Teryaev, Phys. Rev. C **82**, 054910 (2010).